A Channel-Dropping Filter in the Millimeter Region Using Circular Electric Modes*

E. A. J. MARCATILI†, MEMBER, IRE

Summary—**A channel-dropping filter in the millimeter region that transfers TE°_{01} to $TE^{\square}_{10}$ is described and analyzed. The important features are the use of $TE^{\circledcirc}_{011}$ mode in the resonant cavities combined with a mode-selective coupling between circular symmetric and rectangular waveguides which make both heat loss and mode conversion low. Design formulas and experimental results on a model filter centered at 56 kMc are included. Finally, several possible mode transducers and filters based on the idea of mode-selective coupling are described.**

Introduction

THE long-distance waveguide communication system[1] will require the separation of many bands, each several hundred Mc wide, in the region of 35 to 75 kMc. The transmission from repeater to repeater will be made using the low-loss circular electric mode TE°_{01}, but the microwave circuitry at each repeater station will use the $TE^{\square}_{10}$ mode. Consequently, it is convenient to combine the filtering and transducing of modes in a single low-loss operation.

Insertion loss has three sources: mode conversion, heat loss and reflection.

Mode conversion must be kept very low not only because of the insertion loss but also because of possible unwanted resonances of spurious modes.

Heat losses can be minimized using cavities that resonate with high intrinsic Q; this demands the use of circular electric modes in the cavities and a structure that does not require soldering.

Finally, the filters have to be of the constant resistance type in order to permit stacking tens of them, without impairing through multiple reflections the channels to be dropped last.

This paper describes a filter that satisfies all the above conditions and also has the advantages of compactness and convenient spatial orientation of the ports.

The derivations were made having in mind a single pole branching filter, but they are also applicable to the design of maximally flat filters.[2]

As by-products of the filter, several possible transducers from single-mode rectangular waveguide to round waveguide are described. These transducers may be useful for measuring purposes.

* Received by the PGMTT, October 3, 1960; revised manuscript received, December 13, 1960.

† Bell Telephone Labs., Inc., Holmdel, N. J.

[1] S. E. Miller, "Waveguide as a communication medium," *Bell Sys. Tech. J.*, vol. 33, pp. 1209–1265; November, 1954.

[2] G. Goubau, "Electromagnetische Wellenleiter und Hohlraume," Wissenschaftliche Verlagsgesellschaft M.B.H., Stuttgart, Ger.; 1955.

Description of the Filter

In order to understand the behavior of the filter and the reasoning by which the final structure was adopted, consider the schematic circuit in Fig. 1. Because of the proper selection of normalized reactances, the impedance seen towards the right of the plane AA is 1 at all frequencies. At midband frequency the maximum power available goes to R_a and far from resonance it goes to R_b.

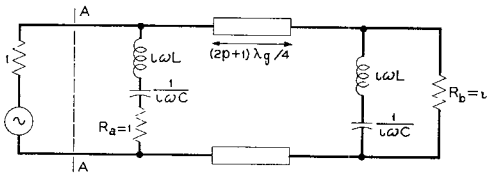

Fig. 1—Low-frequency channel-dropping filter.

The passage from the low-frequency circuit to a microwave circuit is not unique, but an obvious way appears in Fig. 2. The resonators in Fig. 1 have been replaced with the cavities that resonate with the coaxial circular electric mode TE°_{011}.

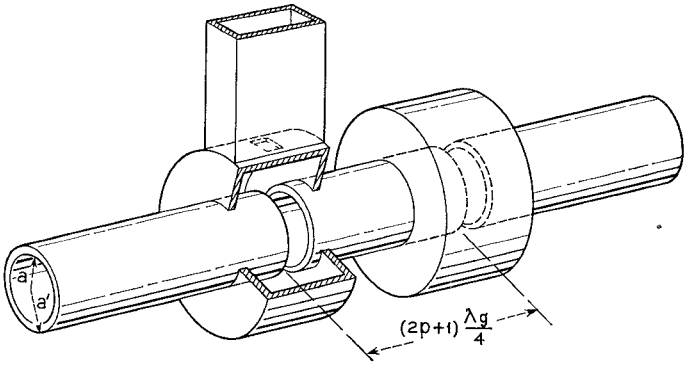

Fig. 2—Microwave channel-dropping filter.

The coupling from the first cavity to an outgoing rectangular waveguide is provided by a hole. This introduces a substantial asymmetry in the otherwise circular symmetric structure, and the first cavity resonates with unwanted spurious modes at frequencies below and above the wanted TE°_{011} mode.

The spurious resonances can be avoided by distributing the coupling from the coaxial cavity to the rectangular waveguide as indicated in Figs. 3(a) and 3(b). An

E-plane T junction in rectangular waveguide has been wrapped around the coaxial cavity. Imagine for the time being that there is no coupling between the rectangular waveguide and the coaxial cavity and that a wave enters the T junction. The standing electric field is antisymmetric with respect to the plane BB and consequently at point 1 has to be zero. This implies that the magnetic field parallel to the axis of the cavity is maximum. At points 2, 3, and 4 located at distances 1, 2 and 3 guided wavelengths from point 1 and measured in the rectangular waveguide, the magnetic fields are also maxima and in phase with that in 1. If now coupling holes are opened in those points, excitation for $TE^{\circledcirc}_{0mn}$, $TE^{\circledcirc}_{7mn}$, $TE^{\circledcirc}_{14mn}$, etc. is provided. By proper selection of the dimensions, the cavity may be made to support only TE_{011} for frequencies smaller than those dropped, and the multimode resonances are avoided.

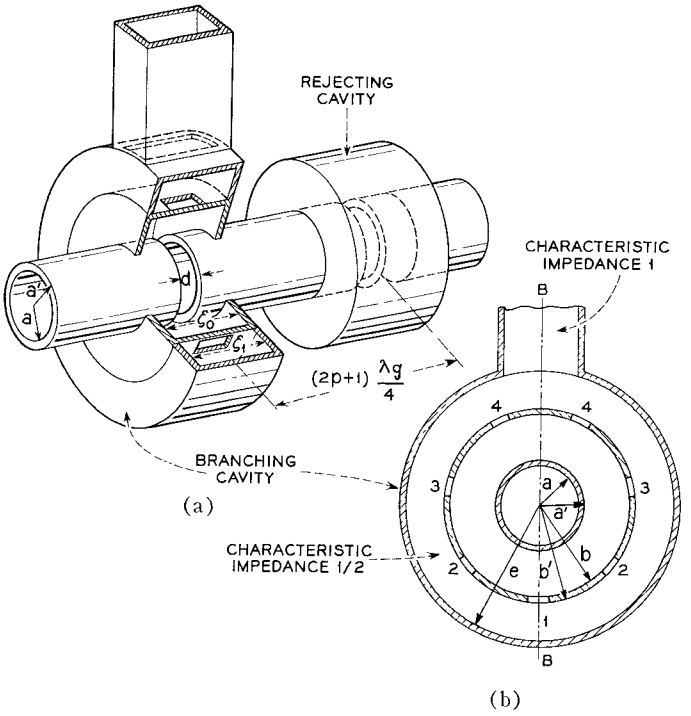

Fig. 3—Mode conversion-free channel-dropping filter.

Another way of looking at the problem of multimode resonances consists in calculating the amount of coupling between the exciting $TE^{\circledcirc}_{011}$ mode and the other coaxial spurious modes. That coupling is proportional to

$$\int_s \overline{H^{\circledcirc}_{011}} \cdot \overline{H^{\circledcirc}_{sp}}\, ds$$

where the vectors $\overline{H^{\circledcirc}_{011}}$ and $\overline{H^{\circledcirc}_{sp}}$ are the magnetic fields of the unperturbed exciting and coupled modes and the integration is extended over the coupling aperture S.[3] In the structure of Fig. 2 the integral is finite, but in that of Fig. 3 the integral tends to zero either because $\overline{H^{\circledcirc}_{sp}}$ is periodic or because the scalar product is null.

[3] H. A. Bethe, "Theory of diffraction by small holes," *Phys. Rev.*, vol. 66, pp. 163–182; October, 1944.

Resume of Design Formulas

In this section, we specify the design formulas. Their derivation is detailed in the Appendix.

In general, the requirements for a filter specify the midband frequency and bandwidth. Alternatively, the requirements may be expressed in terms of λ, midband free space wavelength and Q_L, loaded Q.

The dimensions a, a', b, b', d, e, ζ_0, and ζ_1 in Fig. 3, and c in Fig. 4, are the unknowns.

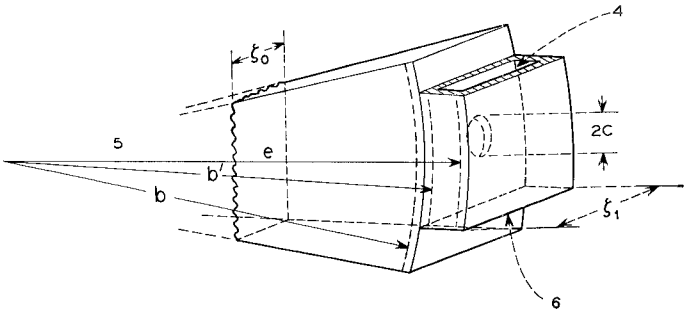

Fig. 4—Elemental outer junction.

Selecting $e-b'/\zeta_1=\frac{1}{2}$, which is the usual aspect ratio of rectangular waveguides, and calling ξ the aspect ratio $b-a'/\zeta_0$ of the coaxial cavity, it follows from (1), (2), (4), (5), (7), (13), (14), and (18), that

$$\frac{\zeta_0}{\lambda} = \frac{1}{2\xi}\sqrt{1+\xi^2}\,(1+\Delta)$$

in which

$$\Delta = \frac{3}{8\pi^2}\frac{\left(\frac{\lambda}{2a}\right)^2}{K} + 3.832\left(\frac{\lambda}{4\pi a}\right)^{3/2}\frac{1}{\left[1-\left(\frac{3.832\lambda}{2\pi a}\right)\right]^{1/4} Q_L^{1/2}} + \sqrt{1-\left(\frac{n\lambda}{2\pi aK}\right)^2}\left(\frac{n}{\pi\xi Q_L}\right)^{1/2}$$

$$K = 1+\frac{\lambda}{2a}\sqrt{1+\xi^2}$$

and n is the number of coupling holes between coaxial cavity and rectangular waveguide. From (4), (5) and (18),

$$\frac{d}{a} = \left[\frac{16}{3.832^2\pi}\frac{\lambda}{a}\sqrt{1-\left(\frac{3.832\lambda}{2\pi a}\right)^2}\,\frac{(1+\xi^2)^2}{\xi}\,\frac{1}{Q_L}\right]^{1/4} \cdot \left[1-\frac{\Delta}{2}(1-\xi^2)\right] + \pi\frac{a'-a}{2a}.$$

From (2), (4), (5), (7), (11) and (13),

$$\frac{2c}{a} = \left[\frac{9\pi}{16n^3}\left(\frac{\lambda}{a}\right)^4 \frac{K^2}{1-\left(\frac{n\lambda}{2\pi aK}\right)^2}\,\frac{(1+\xi^2)^2}{\xi Q_L}\right]^{1/6} \cdot \left\{1+\frac{\Delta}{3}(1-\xi^2)+\frac{\gamma}{3}\left[2-\left(\frac{2\pi aK}{n\lambda}\right)^2\right]\right\} + 1.841\,\frac{2}{3}\,\frac{b'-b}{a}$$

where

$$\gamma = \frac{\dfrac{\lambda}{8aK\sqrt{1-\left(\frac{\lambda n}{2\pi aK}\right)^2}} + (1+\xi^2)\sqrt{1-\left(\frac{n\lambda}{2\pi aK}\right)^2}\,\frac{1}{(n\pi\xi Q_L)^{1/2}} + \frac{\lambda}{2a}\,\frac{(1+\xi^2)^{1/2}\Delta}{K}}{\left(\frac{2\pi aK}{n\lambda}\right)^2 - 1}.$$

In the expressions for d/a and $2c/a$, the corrections due to wall thickness are given by the last terms.

From (6) and (11),

$$\frac{\zeta_1}{\lambda} = \frac{1-\gamma}{2\sqrt{1-\left(\frac{\lambda n}{2\pi aK}\right)^2}}.$$

Finally, from (19), the intrinsic Q of the coaxial cavity results in

$$Q_i = \frac{\pi}{4}\sqrt{120\lambda g}\,\frac{(1+\xi^2)^{3/2}}{1+\xi^3}$$

where g, the conductivity of the metal, and λ are given in mks units. The intrinsic Q passes through a maximum for $\xi=1$, that is, when the cross section of the coaxial cavity is a square.

Experimental Results

A model filter made of silver has been constructed for operation at 56 kMc [Figs. 5(a) and 5(b)]. The performance is shown in Fig. 6. The 3-db bandwidth of the dropped channel is 185 Mc, the insertion loss at midband is 1.4 db and the return loss, measured from 50 to 60 kMc, is larger than 19 db.

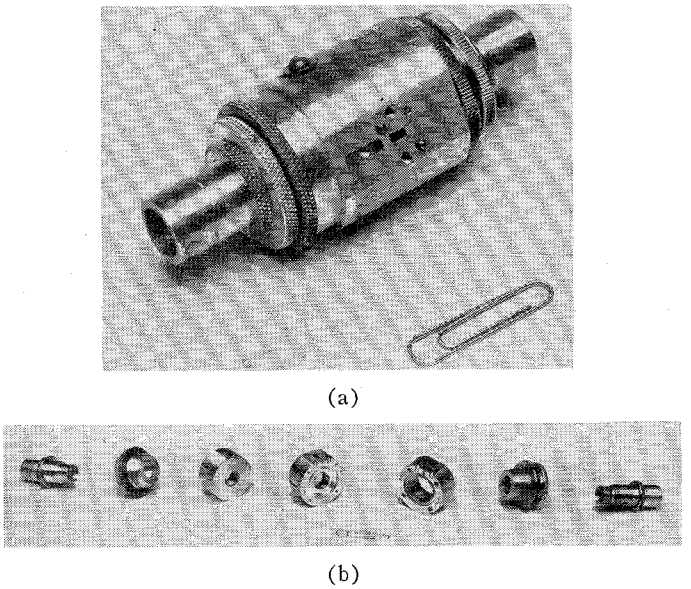

Fig. 5—(a) Channel-dropping filter. (b) Exploded view of channel-dropping filter.

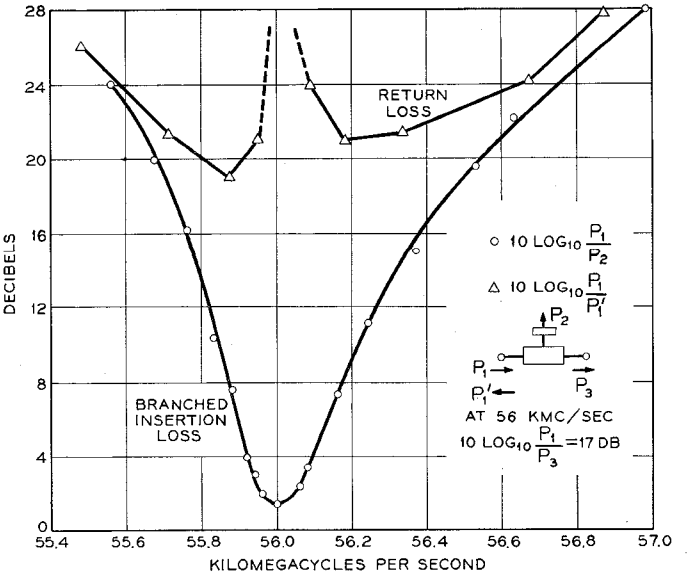

Fig. 6—Experimental results obtained with the channel-dropping filter.

From the measured Q_L and the midband insertion losses in the dropped channel and through waveguide, the intrinsic Q's of the cavities turn out to be

Q_i branching cavity = 2420
Q_i rejecting cavity = 4090.

The theoretical value for both cavities is 6400. The larger loss of the branching cavity is due to the heat dissipation in the multiple coupling holes and in the wrapped rectangular waveguide.

For comparison purposes, it is interesting to know that the measured intrinsic Q of a silver cavity made with 98U waveguide resonating in the $TE^{\square}_{101}$ mode at 5.4 mm is 1000.

Because of the narrow gap providing the coupling between the circular waveguide and the cavities, the return loss of the filter is small, particularly out of resonance. This characteristic makes this filter very attractive when many of them must be stacked together.

Other Transducers

Following the idea of mode-selecting coupling, it is possible to devise many transducers. For example, if in Fig. 3(b) the coupling holes are displaced $\lambda_g/4$, Fig. 7 is obtained. Now the mode excited is circular magnetic and the filter transduces $TE^{\square}_{10}$ to TM°_{01}.

Another example. Using only two holes diametrically opposed coupling electrically in opposite phases, the filter transduces $TE^{\square}_{10}$ to TE°_{11}.

If the resonant cavities are eliminated, Figs. 8 and 9 are obtained. In general, they no longer represent matched narrow-band devices; they become broad-band mismatched mode transducers.

The wrapped-around rectangular waveguide may be located at the end of a round pipe and the holes may be in the broad wall side as in Fig. 10. Circular magnetic modes are excited. The cavity limits the bandwidth but decreases the insertion loss.

The reader can image many more combinations.

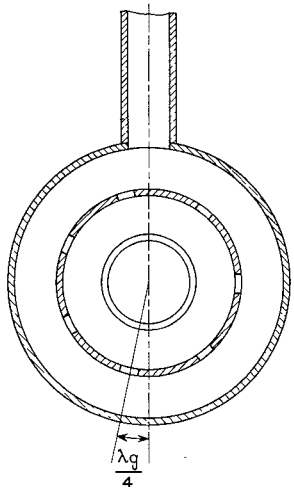

Fig. 7—Matched $TE^{\square}_{10}$ to TM°_{01} transducer.

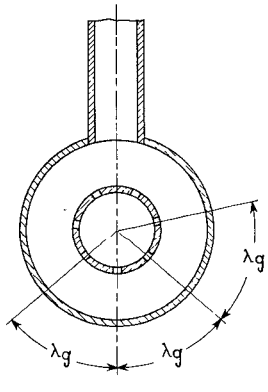

Fig. 8—Mismatched $TE^{\square}_{10}$ to TE°_{01} transducer.

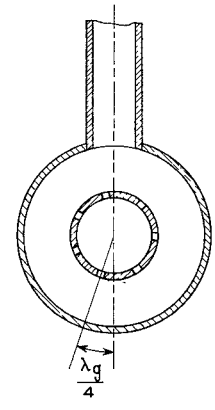

Fig. 9—Mismatched $TE^{\square}_{10}$ to TM°_{01} transducer.

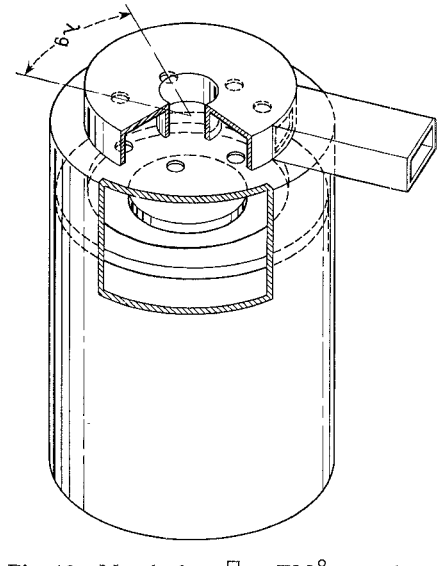

Fig. 10—Matched $TE^{\square}_{10}$ to TM°_{0n} transducer.

Conclusions

A channel-dropping filter capable of transducing TE_{01}° into $TE_{10}^{\square}$ has been described and analyzed. Circular electric modes in the resonant cavities combined with a mode-selective coupling between circular symmetric and rectangular waveguides make both heat loss and mode conversion low. Design formulas and experimental results on a model centered at 56 kMc are included. Because of the narrow gap providing the coupling between the circular waveguide and the cavities, the return loss of the filter is very small, particularly out of resonance. This property, together with the low insertion loss, makes the filter attractive when many of them must be stacked together.

Appendix

Design Formulas

We start analyzing each of the elementary structures that constitute the branching cavity of Fig. 3 and the conditions they must satisfy in order to resonate and to provide the proper bandwidth. Throughout all the following calculations, the arguments of the Bessel functions are large enough to justify asymptotic expansions.

A. Inner Junction, Fig. 11

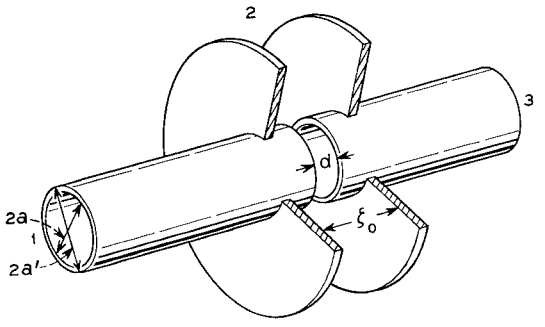

Fig. 11—Inner junction.

This consists of a circular waveguide carrying TE_{01}° and cutoff for TE_{02}°, coupled through a gap to a radial waveguide. Because of symmetry, reciprocity and small coupling, the scattering matrix for this three-port junction is

$$\begin{vmatrix} S_{11} & S_{12} & 1+S_{11} \\ S_{12} & S_{22} & S_{12} \\ 1+S_{11} & S_{12} & S_{11} \end{vmatrix}.$$

The reference surfaces are the plane of symmetry and the cylindrical surface defined by $r=a$.

S_{11} and S_{12}, calculated from small hole theory[3] have moduli small compared to 1. Neglecting powers of S_{11} and S_{12} bigger than 2, S_{22} is obtained from the relations of conservation of energy,[4]

$$S_{11} = i\frac{X_1^2}{32}\frac{d^2\lambda_g}{a^3} \tag{1}$$

$$S_{12} = -\frac{\pi^{1/2}X_1X_2^{1/2}}{8\sqrt{2}}\left(\frac{\lambda_g}{\zeta_0}\right)^{1/2}\left(\frac{d}{a}\right)^2 \tag{2}$$

$$S_{22} = (-1 + |S_{12}|^2)e^{-2S_{11}} \tag{3}$$

where $X_1=3.832$ is the first root of $J_1(x)$.

$$\lambda_g = \frac{\lambda}{\sqrt{1-\left(\frac{3.832\lambda}{2\pi a}\right)^2}} \tag{4}$$

is the midband wavelength in the round waveguide

$$X_2 = \frac{2\pi}{\lambda}a'\sqrt{1-\left(\frac{\lambda}{2\zeta_0}\right)^2}. \tag{5}$$

λ is the midband free space wavelength.

B. Outer Junction, Fig. 12

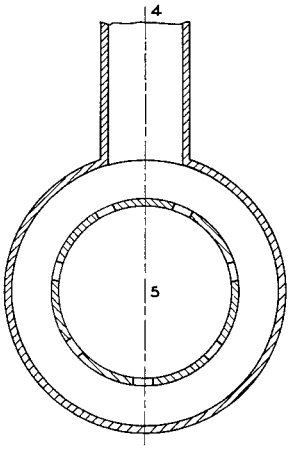

Fig. 12—Outer junction.

This is made out of a radial waveguide carrying a circular symmetric mode coupled through discrete holes to a rectangular waveguide carrying $TE_{10}^{\square}$.

In the description of the filter, it was shown that the holes couple only magnetically. This consideration plus the fact that circular electric modes are unaffected by radial metallic infinitely thin sheets allows one to imagine the junction in Fig. 12 made of n symmetrical three-port structures such as those indicated in Fig. 4.

[4] N. Marcuwitz, "Waveguide Handbook," M.I.T. Rad. Lab. Ser., McGraw-Hill Book Co., Inc., New York, N. Y., vol. 10, pp. 106–108; 1951.

Again using small hole theory, symmetry, reciprocity and conservation of energy, we obtain the elements of the scattering matrix of the junction in Fig. 4. The reference surfaces are the plane of symmetry that contains the round waveguide axis and the cylindrical surface defined by $r=b$.

$$S_{44} = i\frac{16\pi}{3}\frac{c^3}{\lambda_{g1}b'\zeta_1\left[\left(\frac{e}{b'}\right)^2-1\right]} \tag{6}$$

$$S_{45} = -\frac{16\pi}{3}\frac{c^3\left[1-\left(\frac{\lambda}{2\zeta_0}\right)^2\right]^{1/4}}{[(e-b')\zeta_1\zeta_0\lambda]^{1/2}\lambda_{g1}} \tag{7}$$

$$S_{55} = (-1+|S_{45}|^2)e^{-2S_{44}} \tag{8}$$

where ζ_1 is the width of the rectangular waveguide, λ_{g1} the midband wavelength measured along the curved axis of the guide, and $4c^3/3$ the polarizability of the circular coupling hole. If the hole is rectangular, and elongated in the direction of the magnetic field, its polarizability can be found in the literature.[5]

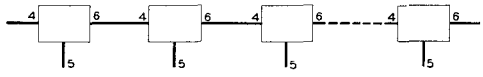

Fig. 13—Equivalent outer junction.

Connecting n such structures together (Fig. 13) and considering that all terminals 5 form a single port in which power adds and that end terminals 4 and 6 form a single port in which power also adds, it is possible to ascertain the scattering matrix elements of the two-port junction in Fig. 12.

$$\Gamma_{45} = (2n)^{1/2}|S_{45}| \tag{9}$$

$$\Gamma_{55} = (-1+n|S_{45}|^2)e^{-2nS_{44}}. \tag{10}$$

The wrapped waveguide must maintain the coincidence of zero electric field with each hole. Therefore, the number of holes, n, is equal to the number of guided wavelengths in the wrapped waveguide. Accordingly,

$$e = \frac{n\lambda\left(1+i\frac{S_{44}}{\pi}\right)}{\pi\sqrt{1-\left(\frac{\lambda}{2\zeta_1}\right)^2}} - b'. \tag{11}$$

The small correction $i(S_{44}/\pi)$ accounts for the lumped reactances introduced by the coupling holes.

[5] S. B. Cohn, "Determination of aperture parameters by electrolytic-tank measurements," PROC. IRE, vol. 39, pp. 1416–1421; November, 1951.

C. Resonance Conditions

At midband the rejecting cavity provides an open circuit at the input of the branching cavity. In order to have complete transfer of power through the branching cavity, the reflection coefficients seen looking away from each side of a reference surface must be complex conjugates. If that reference is the cylinder of radius $r=a'$ (Fig. 3), the following condition is obtained,

$$S_{22}^* = (-1+2|S_{12}|^2)e^{+2S_{11}} = \left[\frac{H_1^{(1)}(X_2)}{H_1^{(1)}\left(X_2\frac{b}{a}\right)}\left|\frac{H_1^{(1)}\left(X_2\frac{b}{a}\right)}{H_1^{(1)}(X_2)}\right|\right]\Gamma_{55}, \tag{12}$$

where the asterisk means complex conjugate of. The Hankel functions $H_1^{(1)}$ appear because of the radial line of length $b-a'$ connecting the junctions in Figs. 11 and 12. Replacing the value of Γ_{55} with the one obtained in (10), equating moduli and arguments, and using asymptotic expansions for the Hankel functions, the following expressions are found

$$|S_{12}| = \left(\frac{n}{2}\right)^{1/2}|S_{45}| \tag{13}$$

$$\frac{b}{a'} = 1+\frac{\pi}{X_2}+\frac{3\pi}{8X_2^3}\frac{1}{1+\frac{\pi}{X_2}}-\frac{S_{11}+nS_{44}}{iX_2}. \tag{14}$$

For the rejecting cavity, the condition of resonance is fulfilled when the arguments of the two reflection coefficients are equal and of opposite sign. Consequently, from (14),

$$\frac{\bar{b}}{a'} = 1+\frac{\pi}{\bar{X}_2}+\frac{3\pi}{8\bar{X}_2^3}\frac{1}{1+\frac{\pi}{\bar{X}_2}}-\frac{\bar{S}_{11}}{i\bar{X}_2} \tag{15}$$

where the dashed letters refer to dimensions in the rejecting cavity.

D. Q of the Cavities

We start considering the different loaded Q's that can be found in the circuit shown in Fig. 1. The voltage at AA is frequency independent and therefore the prescribed dropped channel's Q is $Q_L=\sqrt{L/C}$.

For measuring purposes, it is important to realize what are the loaded Q's of the two cavities when they are considered separately. In Fig. 1, if the branching cavity doesn't exist, the loaded Q of the rejecting cavity is $2Q_L$. On the other hand, if the rejecting cavity doesn't

exist, the branching cavity has a loaded Q equal to $\frac{2}{3}Q_L$ and it is not matched. At midband, entering in any port, the normalized reflected power is 1/9 and the normalized transmitted power to each of the other two ports is 4/9.

By definition, the Q of a cavity is

$$Q = \frac{w\omega}{P} \tag{16}$$

where w is the energy stored in the cavity, ω is the angular frequency and P is the power leaving the cavity.

The loaded Q of either cavity when they are operating together, that is, the Q measured in the dropped channel is

$$Q_L = \frac{w\omega}{4|S_{12}|^2 P_i} \tag{17}$$

where P_i is the power carried by either of the two radially propagating waves that build the standing wave in each cavity. The calculation is straightforward and

$$Q_L = \frac{256\pi}{X_1^2 X_2^2} \frac{\zeta_0}{\lambda_g} \frac{a'^2}{\lambda^2} \left(\frac{b}{a'} - 1\right)\left(\frac{a'}{d}\right)^4. \tag{18}$$

The intrinsic Q of a cavity is obtained from (16) when P is the power dissipated in the walls, and the result is

$$Q_i = \frac{2(b - a')^3}{\delta\lambda^2} \frac{1}{1 + \left(\frac{b - a'}{\zeta_0}\right)^3}. \tag{19}$$

$\delta = \sqrt{2/\omega\mu g}$ is the skin depth, ω is the angular frequency, μ the permeability and g the conductivity of the metal.

Eqs. (18) and (19) may be applied to either of the cavities by choosing the appropriate dimensions given in (14) and (15).

Coupled-Mode Description of Crossed-Field Interaction*

J. E. ROWE†, MEMBER, IRE, AND R. Y. LEE†

Summary—**The coupled-mode theory is developed for two-dimensional M-type flow, and a system of five coupled-mode equations is obtained. A fifth degree secular equation is found for the perturbed propagation constants of the system. Under weak space-charge field conditions, both the forward-wave and backward-wave interactions may be described in terms of only two coupled modes. The two-mode theory is applied to the calculation of starting conditions for the M-BWO, and to the M-FWA. The conditions for beating-wave amplification are determined, and the variation of the mode amplitudes with distance is given.**

Introduction

THE coupled-mode theory has been used extensively to describe the operation of the traveling-wave amplifier and backward-wave oscillator.[1-3] In these analyses, the four mode equations refer to the two beam space-charge waves and the two circuit waves. In both the O-type amplifier and the backward-wave oscillator, the best interaction occurs near synchronism between the slow space-charge wave and the circuit wave, and three waves are sufficient to describe the interaction, the fourth being far out of synchronism with the electron beam. Under large space-charge conditions in O-type devices, the interaction is accurately described by utilizing only the slow space-charge wave and the forward circuit wave. The coupled-mode analysis has great utility in obtaining a clear understanding of the detailed interaction mechanism.

Heretofore, the M-type interaction has not been studied with the coupled-mode theory. The general analysis is somewhat more complicated than that for the O-type, since there are five waves involved, which leads to a fifth-degree secular equation. When the RF structure is matched at its output, and the device is operated near synchronism between the electron beam and the foward circuit wave, the interaction is principally due to two waves. This two-wave interaction occurs for low space-charge conditions, unlike the corresponding conditions in the O-type tube. It is the purpose of this paper to develop the coupled-mode description for planar M-type amplifiers and oscillators and to show how this description may be used to investigate growing-wave gain, beating-wave gain and start-oscillation phenomena.

* Received by the PGMTT, November 29, 1960.

† Electron Physics Lab., Dept. of Elec. Engrg., The University of Michigan, Ann Arbor, Mich. This work was supported by the U. S. Signal Corps under Contract No. DA 36-039 sc-78260.

[1] J. R. Pierce, "Coupling of modes of propagation," *J. Appl. Phys.*, vol. 25, pp. 179–183; February, 1954.

[2] J. R. Pierce, "The wave picture of microwave tubes," *Bell Sys. Tech. J.*, vol. 33, pp. 1343–1372; November, 1954.

[3] R. W. Gould, "A coupled mode description of the backward-wave oscillator and the Kompfner dip condition," IRE TRANS. ON ELECTRON DEVICES, vol. ED-2, pp. 37–42; October, 1955.